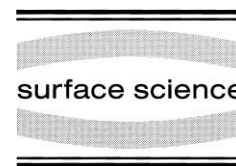




ELSEVIER

Surface Science 412/413 (1998) 192–201



TEM study of tantalum clusters on Al₂O₃/NiAl(110)

S.A. Nepijko^a, M. Klimenkov^a, H. Kuhlenbeck^{a,*}, D. Zemlyanov^b, D. Herein^b,
R. Schlögl^b, H.-J. Freund^a

^a Fritz-Haber-Institut der Max-Planck-Gesellschaft, Abteilung Chemische Physik Faradayweg 4–6, D-14195 Berlin, Germany

^b Fritz-Haber-Institut der Max-Planck-Gesellschaft, Abteilung Anorganische Chemie Faradayweg 4–6, D-14195 Berlin, Germany

Received 23 March 1998; accepted for publication 19 May 1998

Abstract

Employing transmission electron microscopy (TEM), energy dispersive X-ray analysis (EDX) and X-ray photoelectron spectroscopy (XPS) we have studied tantalum clusters on a thin Al₂O₃ film epitaxially grown on NiAl(110). Our data reveal that the clusters are three dimensional, growing epitaxially on the oxide film with their [110] directions parallel to the surface normal and Ta[001]||NiAl[001]. From the observed moiré fringes the tantalum lattice constant could be determined as a function of the cluster size. We found that the lattice constant decreases with decreasing cluster size with the highest observed reduction being 4.5% for a cluster with a diameter of 12.5 Å. Interestingly the clusters are only partly oxidized as concluded from XPS, TEM and EDX data although the samples were exposed to air after cluster deposition. © 1998 Elsevier Science B.V. All rights reserved.

Keywords: Aluminum oxide; Cluster; Energy dispersive X-ray analysis; Tantalum; Thin films; Transmission electron microscopy; X-ray photoelectron spectroscopy

1. Introduction

Metal particles supported on oxide substrates play an important role in the field of heterogeneous catalysis where they act as catalytically active parts of the catalyst. The properties of small particles may differ considerably from those of the bulk material [1]. This concerns the electronic properties of clusters as well as their lattice. Modelling the electrically non-conducting amorphous oxide material used as support material in technical catalysis by thin, sufficiently conducting oxide films allows electron spectroscopy to be applied to well-defined systems without charge compensation.

Therefore all types of electron spectroscopy may be combined with methods well established in the field of technical chemistry such as transmission electron microscopy (TEM). Especially the last method has had a large impact on heterogeneous catalysis in the past [2–5].

We have used a thin aluminum oxide film grown on NiAl(110) as a substrate for particle deposition in the present experiments. This film been characterized in previous studies under UHV (ultra-high vacuum) conditions using several methods such as LEED (low-energy electron diffraction), photoemission and STM (scanning tunneling microscopy) [6–8]. Therefore its properties are well known. After characterization of the clean oxide film we have studied deposited metal clusters such as platinum, palladium, rhodium

* Corresponding author. Fax: +49 30 8413 4307;
e-mail: Kuhlenbeck@FHI-Berlin.MPG.DE

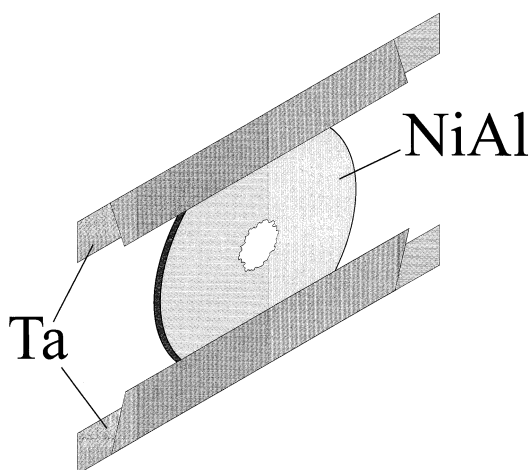


Fig. 1. Schematic drawing of the NiAl(110) sample used for the experiments.

and silver [9–12]. These investigations revealed pronounced differences between the properties of the bulk material and the clusters concerning electron structure as well as geometry and adsorption.

In a previous TEM study of platinum clusters on $\text{Al}_2\text{O}_3/\text{NiAl}(110)$ [13] we have shown that the lattice constant of the clusters depends on their size. For $\text{Pt}/\text{Al}_2\text{O}_3/\text{NiAl}(110)$ we could also demonstrate that neither the oxide film nor the clusters are significantly modified by contact with air. In the present case we will report on tantalum clusters which are expected to be chemically much less inert than platinum clusters.

2. Experimental

The Al_2O_3 films were prepared by oxidation of an NiAl(110) single crystal disk with a thickness of about 0.5 mm and 3 mm in diameter. This sample was cut from a single crystal rod after orientation with Laue backscattering with an accuracy of about $\pm 1^\circ$. After polishing the disk using standard procedures it was etched in a fast ion etching system until a hole with a diameter of about 0.2 mm was formed in the center. The edge

of the hole was wedge shaped with an angle of $5\text{--}10^\circ$ and a thickness of less than 10 Å directly at its boundary thus permitting TEM to be performed in the region near to the hole.

Preparation of the sample, oxidation and cluster deposition were performed in a simple UHV system with a base pressure of about 10^{-10} mbar. It is equipped with facilities for sample preparation and a LEED system for analysis of surface order. The sample was mounted between two strips of tantalum foil (see Fig. 1). Heating was possible by passing an electric current through the strips. The sample was cleaned in UHV by repeated cycles of sputtering with Ar ions (700 eV) at room temperature and annealing at 1300 K. After cleaning and ordering of the sample surface the oxide film was prepared by dosing oxygen (1500 L at 5×10^{-6} mbar) with the sample temperature held at 550 K followed by annealing for some minutes at 1200 K. The oxide film is about 5 Å thick, well ordered and exhibits a complicated LEED pattern. More details of the preparation procedure and the structure of the film may be found in Refs. [6,8]. The tantalum clusters were deposited on the surface during the final flash to 1100 K which was needed to order the oxide film. This led to the evaporation of a small amount of tantalum from the Ta strips.

For the studies two different 200 keV electron microscopes (Hitachi-8100 and Philips CM-200FEG, ultimate lattice resolution in both cases: 1.44 Å) containing facilities for energy dispersive X-ray spectroscopy (EDX) and electron energy loss spectroscopy (EELS), respectively, were used. The double tilt specimen holders of the microscopes allowed for precise positioning and alignment of the sample with respect to the electron beam. During the transfer from the UHV system into the microscope the sample was exposed to air for a few minutes.

The XPS data were obtained in a modified LHS 12 system with MCD (multichannel) detection and facilities for XPS and ISS (ion scattering spectroscopy). Electrons were excited with Mg $K\alpha$ radiation ($h\nu = 1253.6$ eV). For the XPS experiments the analyzer pass energy was set at 108 eV corresponding to a resolution of about 1.2 eV.

3. Results and discussion

3.1. Structure of the tantalum clusters

Fig. 2 exhibits an electron diffraction pattern of the Al_2O_3 film covered with tantalum clusters. The most prominent spots in this figure are due to the NiAl(110) substrate. The Al_2O_3 film grows on NiAl(110) with its [111] direction parallel to the surface normal (for details see Refs. [6,8,14]). Some 440 type spots of the oxide film are located on the dashed circle in Fig. 2.

Fig. 2 exhibits also some diffuse spots due to tantalum clusters which are marked by arrows in

this figure. As deduced from the arrangement of these spots, the lattice of the clusters is of bcc type. The [110] directions of the clusters are oriented parallel to the surface normal and they grow epitaxially on the surface with $\text{Ta}[001] \parallel \text{NiAl}[001]$. The latter point is interesting since this means that the clusters possibly “feel” the structure of the NiAl(110) substrate through the oxide indicating that the NiAl structure influences the structure of the oxide film as has already been discussed in Ref. [8].

Three rectangles are drawn in Fig. 2. The largest one marks spots due to the NiAl substrate with a lattice constant of $a = 2.887 \text{ \AA}$ and the smallest one

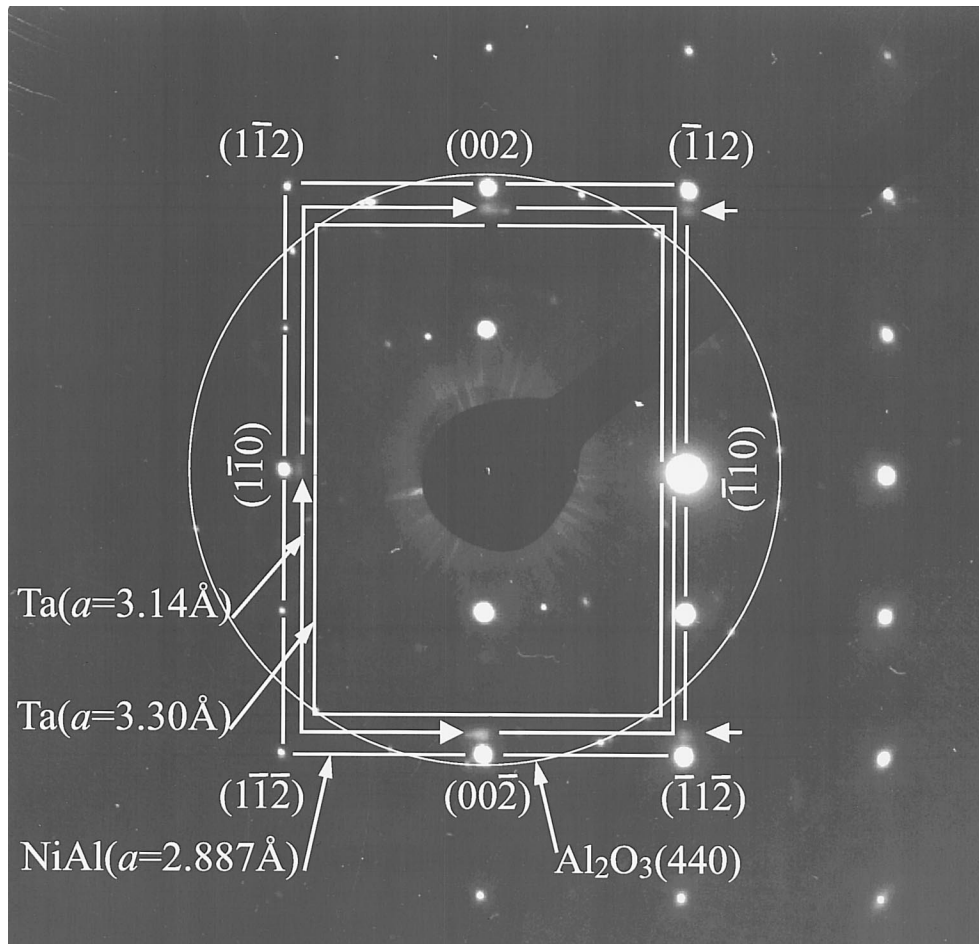


Fig. 2. Electron diffraction pattern of $\text{Al}_2\text{O}_3/\text{NiAl}(110)$ covered with Ta clusters. The image was taken using the electron beam of a transmission electron microscope. Reflections due to the tantalum clusters are marked by arrows.

corresponds to bulk tantalum with a lattice constant of $a = 3.3029 \text{ \AA}$ [15]. Obviously the latter rectangle does not fit the tantalum spots, indicating that the lattice constant of the clusters deviates from that of bulk crystals. A rectangle that fits the spots of the Ta clusters has also been drawn in Fig. 2. It corresponds to a lattice constant of $a \approx 3.14 \text{ \AA}$.

A closer inspection of the diffraction pattern reveals that the Ta($\bar{1}12$) and Ta($\bar{1}1\bar{2}$) spots are not situated on the corners of the rectangle with $a = 3.14 \text{ \AA}$, indicating that these spots are due to dynamic effects (double diffraction). This diffraction involves the reflection pairs NiAl($\bar{1}10$)/Ta(002) and NiAl($\bar{1}10$)/Ta(00 $\bar{2}$). Support is given to this interpretation by the high intensity of the NiAl($\bar{1}10$) spot.

Similar to the case of Pt/Al₂O₃/NiAl(110) [13], for tantalum clusters also moiré fringes due to double diffraction are observed. This is illustrated in Fig. 3 which clearly exhibits clusters with moiré fringes. These patterns are due to diffraction of the electron beam by the NiAl substrate with subsequent scattering by the Ta clusters.

Three different types of moiré fringes have been identified in our TEM images which are listed in Table 1. The reciprocal lattices of the NiAl(110) substrate and the tantalum clusters are drawn in Fig. 4. Also three sets of reciprocal lattice vectors as listed in Table 1 are indicated in this figure [\overline{OAB} (type 1), \overline{OCD} (type 2) and \overline{OFG} (type 3)]. The vectors CD, FG and AB are the k -vectors of the moiré fringes.

There are also cases where two types of moiré fringes are visible on the same cluster as illustrated in Fig. 5a. This pattern has been Fourier trans-

formed yielding maxima in the Fourier transform due to the two types of moiré fringes. After erasing the maxima due to moiré type 3 and back transformation, Fig. 5b was obtained showing only the pattern due to moiré type 1. Similarly Fig. 5c exhibits only the moiré fringes of type 2.

Fig. 6a shows a TEM image where also two sets of moiré fringes are superimposed. However, this time the two patterns are due to different sources, i.e. one is due to a Ta cluster and the other, which is also found in the surroundings of the cluster, is due to the γ -Al₂O₃ film (Al₂O₃ + NiAl double diffraction [14]). This figure is shown in order to prove that the cluster is situated on the oxide film and not directly on the NiAl substrate. Fig. 6b exhibits a Fourier filtered part of Fig. 6a in which both sets of moiré fringes have been enhanced, and for clarity in Fig. 6c the moiré fringes due to the Ta cluster have been deleted so that only the moiré fringes of the oxide are still visible. This pattern also shows up in the area where the cluster is situated so that there must be oxide below the cluster.

The lattice constants of the tantalum clusters may be calculated from the observed moiré fringes. According to Fig. 4 one needs to know the k -vectors of the moiré fringes which may be read off directly from the TEM images and the corresponding k -vectors of the NiAl(110) substrate. From this information the reciprocal lattice vectors of the Ta clusters may be calculated. Assuming that the lattices of the clusters are not distorted too much one may use these vectors to calculate the lattice constants of the clusters. We note that this procedure is not unique at first sight since neither the directions of the moiré k -vectors nor the NiAl reciprocal lattice vectors taking part in the double diffraction process may be obtained directly from the experimental data. Therefore we have tested different combinations of NiAl low index reciprocal lattice vectors and directions of $k_{\text{moiré}}$ considering that the NiAl and Al₂O₃ reflections have to be strong and that the difference of the k -vectors have to be small in order to yield a small value for $k_{\text{moiré}}$ as experimentally observed. A test was considered to be successful when the calculated Ta lattice constant was near to the literature value for tantalum (3.3029 \AA [15]). Since usually all other combinations led to unphysical results we

Table 1
Three types of combinations of NiAl and Ta lattice vectors leading to the moiré fringes observed in our data. For details see Fig. 4

No.	NiAl reciprocal lattice vector	Ta reciprocal lattice vector
1	$\bar{1}10$ type	$\bar{1}10$ type
2	$\bar{1}11$ type	$\bar{1}12$ type
3	002 type	002 type



Fig. 3. TEM image of tantalum clusters (see arrows) on $\text{Al}_2\text{O}_3/\text{NiAl}(110)$.

are sure that the chosen combinations are the correct ones. How the calculations have been performed is described in more detail in Ref. [14].

The result of the calculations is shown in Fig. 7 as a function of the cluster size. This figure shows that the lattice constant decreases with decreasing cluster size with the highest observed reduction being about 4.5% for a cluster size of 12.5 Å. With increasing cluster size the lattice constant asymptotically approaches the value for bulk tantalum (3.3029 Å [15]). The reason for this behavior is that for small clusters the surface energy is a notable part of the total energy which may influence the lattice constant. A similar observation has been made for $\text{Pt}/\text{Al}_2\text{O}_3/\text{NiAl}(110)$ [13] and several other materials [16]. At this point we note that part of the tantalum was oxidized as will be

discussed in more detail below. Therefore the surface energy does not necessarily refer to metallic tantalum in the present case.

For the determination of the tantalum lattice constants displayed in Fig. 7 the NiAl lattice in the TEM images served as a scale. Therefore for an NiAl(110) sample cut from the same NiAl rod as those used in the present study the lattice constant was calibrated using X-ray diffraction (XRD). For the measurement a Stoe & Cie Theta/Theta powder diffractometer equipped with a graphite secondary monochromator was used. The diffraction pattern was taken with $\text{Cu K}\alpha$ radiation. These studies yielded a value of 2.8866(2) Å for the lattice constant of NiAl which agrees well with the value of 2.887 Å given in the JCPDS database (entry number 20-0019).

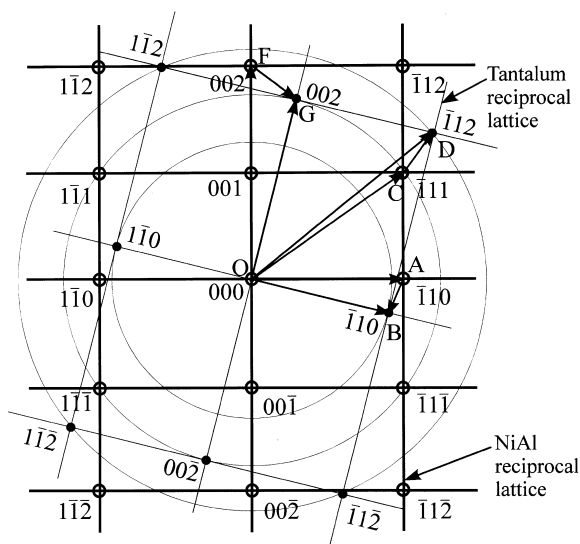


Fig. 4. Schematic drawing of the reciprocal lattices of the tantalum clusters and the NiAl(110) substrate. The angular misalignment of the cluster lattice with respect to the NiAl lattice which is typically in the range of less than 1° is exaggerated here.

Some tantalum clusters were also observed near to the boundary of the NiAl(110) wedge (see Fig. 8). Whether these clusters are in direct contact with the NiAl or whether there is an oxide layer between the clusters and the alloy is not obvious from the images. The cluster displayed in Fig. 8 is rather large (approximately $300 \times 100 \text{ \AA}^2$) and exhibits a well-resolved lattice. In contrast to the clusters observed on the oxide film (Fig. 3) where the Ta[110] direction points along the surface

normal of the sample this one is (100) oriented. The same result has been obtained for other clusters observed at the boundary of the NiAl wedge. A well-resolved moiré-like pattern is visible on the cluster near to the Ta–NiAl (or Ta–Al₂O₃–NiAl) interface [Ta(530)∥NiAl($\bar{1}\bar{1}$)] which could result from a mismatch of the lattices at the interface. This would lead to structural modification near the interface. Of course, in this region double diffraction effects also have to be considered.

3.2. Chemical composition of the tantalum clusters

As already noted, the samples were exposed to air after cluster deposition. For Pt clusters exposure to air did not lead to oxidation [13]. Tantalum is much more reactive with respect to oxide formation so that it was near at hand to investigate the chemical composition of the clusters. A first hint is that the geometric structure of the clusters is near to that of elemental tantalum which excludes heavy oxidation.

We checked the chemical composition of the clusters with EDX and XPS. Two EDX spectra of a cluster with a diameter of 60 \AA are shown in Fig. 9. For the top spectrum a detection area with a diameter of 400 \AA was chosen whereas for the spectrum at the bottom the diameter of the detection area was only 100 \AA . The ratio of the intensities of the oxygen and the tantalum signals is about 1.25 in the top spectrum whereas in the bottom spectrum the oxygen intensity is so small

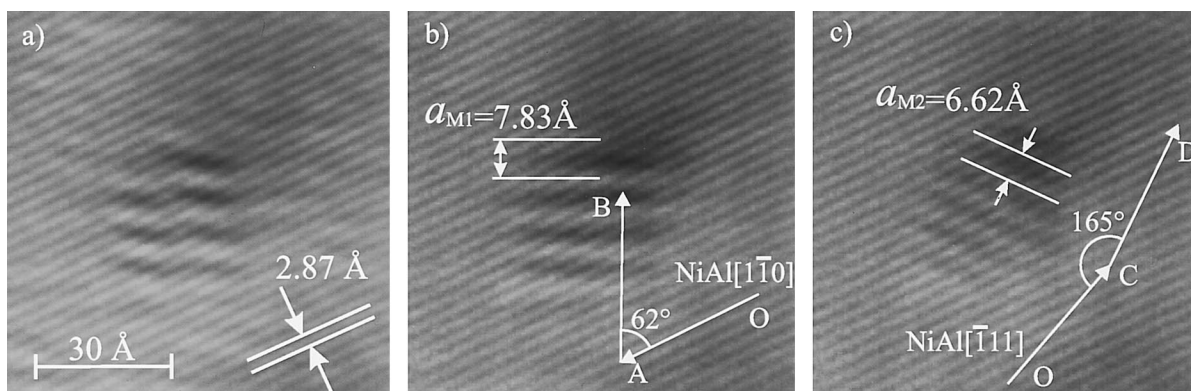


Fig. 5. TEM image of a tantalum cluster on Al₂O₃/NiAl(110). (a) raw data showing two systems of moiré fringes. (b), (c) images obtained after Fourier transformation of (a), erasing of spots due to one type of moiré fringes and back transformation.

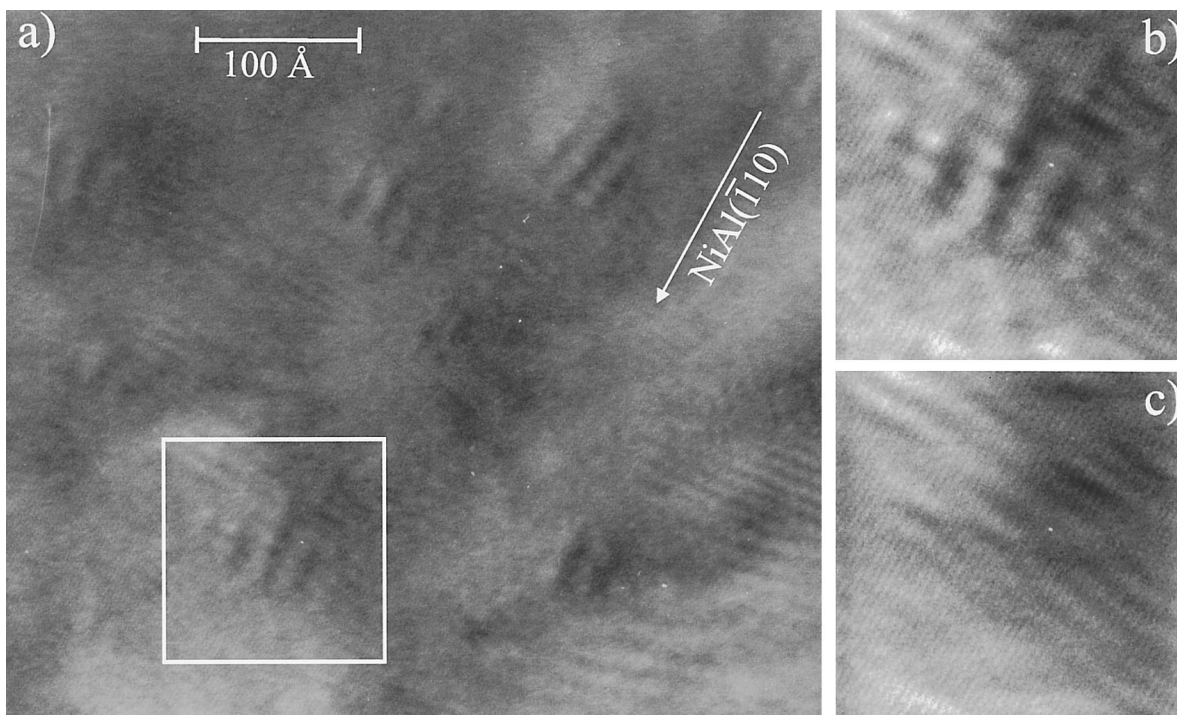


Fig. 6. (a) TEM image of tantalum clusters on $\text{Al}_2\text{O}_3/\text{NiAl}(110)$. (b) Enlarged section of part (a) showing a superposition of moiré fringes due to a Ta cluster and to the Al_2O_3 film. This image has been Fourier filtered. This means that the original image has been Fourier transformed. In the Fourier-transformed image all background intensity was deleted and then the image was transformed back. (c) Similar to (b). In this case not only was the background deleted in the Fourier-transformed image but also maxima due to the moiré fringes of the tantalum cluster so that this image exhibits only the moiré fringes of the Al_2O_3 film.

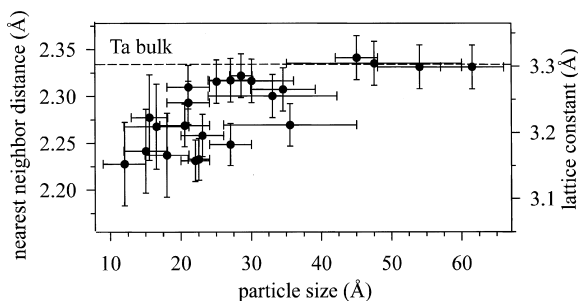


Fig. 7. Dependence of the tantalum lattice constant on the particle size. The horizontal lines indicate the sizes of the small and the long sides of the clusters. The vertical bars give the estimated errors for the calculated lattice constants.

that the intensity ratio may not exceed a value of 0.1. Thus the decrease of the oxygen intensity follows roughly that of the detection area (1/16). This means that this signal must be mainly due to the oxide below the cluster and only a small

amount of oxygen may be contained in the cluster. In view of the limited statistics of the data it is not possible to make a quantitative statement. However, it is clear that the amount of oxygen contained in the cluster is far too low for a regular tantalum oxide.

The chemical composition of the Ta clusters has also been studied using XPS. A set of data exhibiting the 4f levels of the Ta clusters is shown in Fig. 10. According to literature data the Ta $4f_{7/2}$ and $4f_{5/2}$ binding energies of bulk tantalum are 21.6 and 23.5 eV, respectively [17]. The levels of pure, thick Ta_2O_5 should be visible at about 5.5 eV higher binding energies [18]. According to Ref. [18] there are three additional 4f states corresponding to tantalum suboxides. These are shifted by approximately 0.5, 1.2 and 2 eV to higher binding energies with respect to the lines of unoxidized tantalum. In the present case the binding

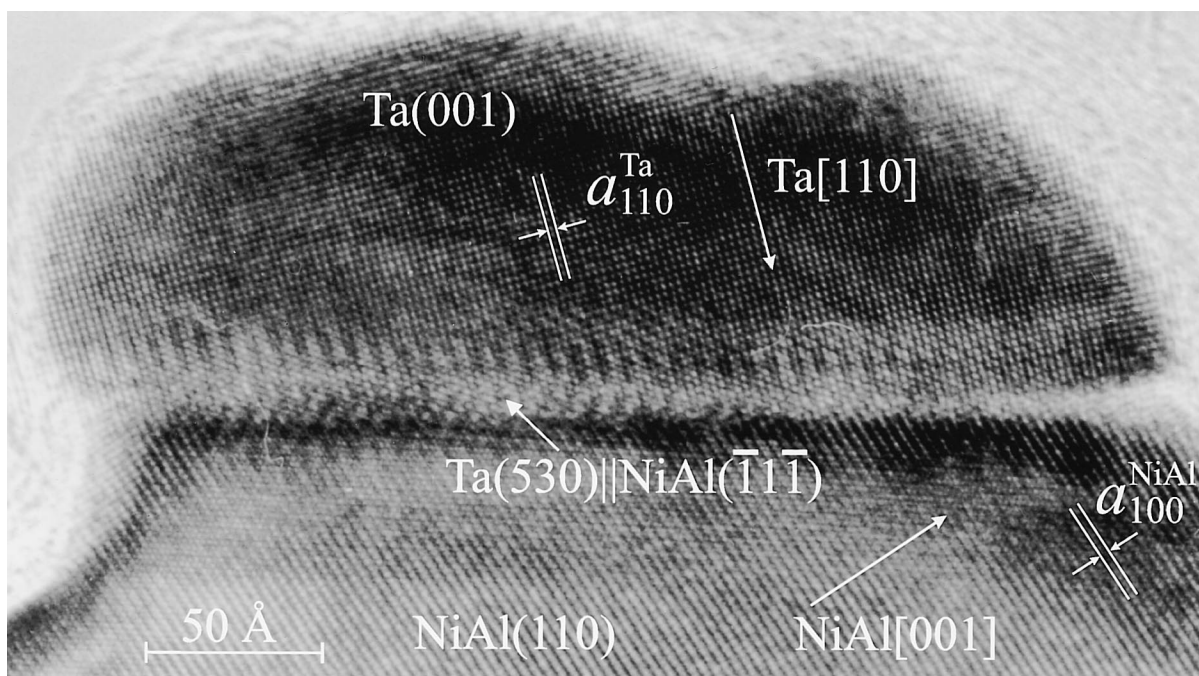


Fig. 8. HRTEM image of a tantalum cluster at the periphery of the NiAl(110) wedge.

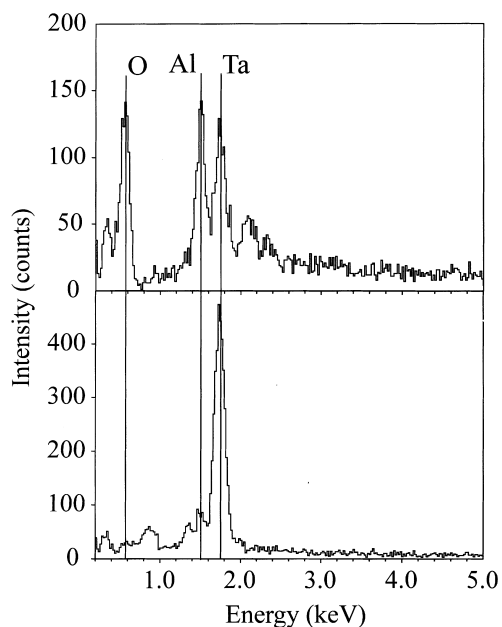


Fig. 9. EDX spectra of a tantalum cluster with a diameter of 60 Å on $\text{Al}_2\text{O}_3/\text{NiAl}(110)$. Top spectrum: 400 Å diameter detection area. Bottom spectrum: 100 Å diameter detection area.

energies of the 4f main lines are 22.6 and 24.5 eV (see Fig. 10). These values are about 1 eV higher than the literature values for elemental Ta. Here two possible reasons have to be discussed:

- (1) The binding energies are shifted owing to the limited sizes of the clusters. In this context we note that the lattice constants of the clusters are reduced with respect to the value for bulk tantalum. This induces modifications of the electronic properties of the clusters which might shift the core level binding energies. Another point is that the positive charges of the core holes in small clusters may only delocalize into the limited volume of the cluster. This will move the core levels to higher binding energies with the shift being dependent on the cluster size [19,20]. In Refs. [10,21] it has been shown that this type of energy shift of core levels for metal deposits on $\text{Al}_2\text{O}_3/\text{NiAl}(110)$ may reach values of about 1 eV.
- (2) The surfaces of the clusters may be covered by suboxides. According to Ref. [18] this would lead to a shift of the main features to higher binding energies.

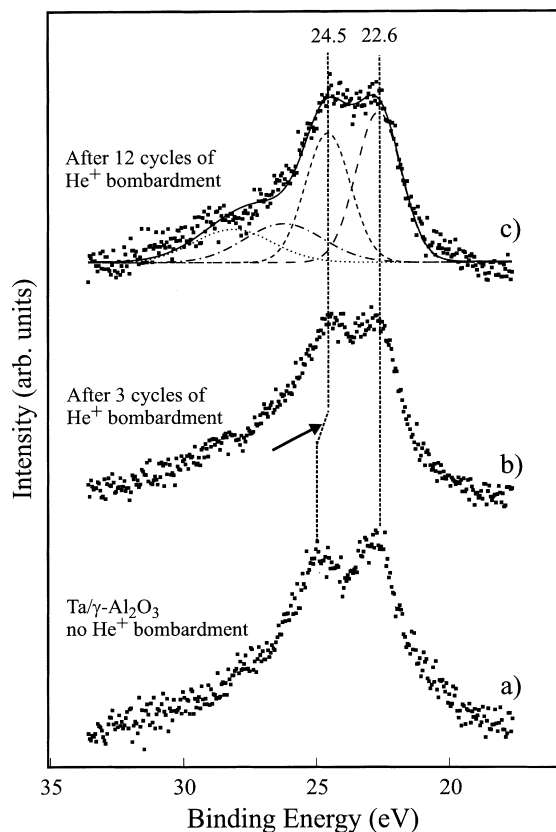


Fig. 10. XPS spectra of the 4f levels of tantalum clusters on $\text{Al}_2\text{O}_3/\text{NiAl}(110)$. (a) spectra taken before He^+ bombardment. (b), (c) spectra recorded after He^+ irradiation. One cycle corresponds to 3 min of bombardment with He^+ ions with a kinetic energy of 1000 eV and a current density at the sample surface of $6 \mu\text{A cm}^{-2}$.

As indicated by the data presented in Fig. 9 there may be only a small amount of oxygen contained in the Ta deposits. Therefore the shift of the core levels must be mostly due to the limited sizes of the clusters and not to oxidation. This interpretation is corroborated by XPS spectra of the 4f levels obtained after bombardment with He^+ ions (Fig. 10). The ion intensity has been chosen such that three cycles of bombardment removed one Ta layer from the cluster. The data presented in Fig. 10 show that after removal of one Ta layer the 4f-derived features shift slightly to lower binding energy. Removal of three additional layers does not shift the 4f levels any more.

This observation indicates that on the surface of the cluster only a small amount of oxygen is found. The oxygen may be removed by sputtering off just one layer since further sputtering does not shift the peaks any further, demonstrating that only a (sub)monolayer amount of oxygen may be contained on the cluster surface.

The spectra displayed in Fig. 10 also exhibit a feature around 29 eV binding energy which is to be attributed to Ta_2O_5 [18]. According to the fitting curves drawn in Fig. 10c the intensity amounts to about 30% of the total intensity so that 30% of the tantalum on the sample surface must be fully oxidized. The intensity did not decrease significantly upon sputtering with He^+ ions which is probably due to the different alignments of the analyzer and the ion bombardment gun. Therefore the gun was not able to reach all places on the surface visible to the analyzer.

The finding that the tantalum clusters survived the transport through air without getting strongly oxidized is somewhat surprising since tantalum is known to react strongly with oxygen [18,22]. A similar inertness with respect to oxidation has been reported previously for platinum clusters [13]. One might assume that this is due to inherent properties of clusters. However, finely dispersed metal is usually very reactive with respect to oxidation so that this explanation must be rejected. Another explanation is that the interaction with the oxide somehow protects the clusters from oxidation. A possible mechanism may be that the cluster-substrate interaction is smaller for Ta_2O_5 than for Ta, which would make oxidation energetically unfavorable. It may also be the case that additional activation barriers for oxidation exist near the interface. At least in this region this would protect the tantalum from being oxidized or slow down the oxidation rate.

Another piece of information contained in the XPS spectra shown in Fig. 10 is that the average thickness of the cluster is much larger than 4 monolayers since the intensity of the 4f levels is not influenced significantly by the removal of four layers with ion bombardment. This is a clear indication that the clusters on the surface are three dimensional. Therefore it may be the case that the

observed XPS signals from Ta₂O₅ in Fig. 10 result predominantly from the top parts of the clusters. These parts are expected to be less protected from oxidation since here the cluster–substrate interaction will have only a weak influence.

4. Summary

In the present paper we report on tantalum clusters on Al₂O₃/NiAl(110). As observed before for platinum clusters on this oxide film we find that the Ta lattice constant decreases with decreasing cluster size with the highest observed reduction being 4.5% for a cluster size of about 12.5 Å. Such an effect has also been observed for some other metallic clusters [13,16] and is most likely due to the increase of the ratio of the number of surface atoms to the total number of atoms in the cluster with decreasing cluster size. The clusters are three dimensional with their (110) directions pointing along the surface normal and Ta[001]||NiAl[001].

Interestingly the clusters are not strongly oxidized upon contact with air. This is unexpected since tantalum reacts strongly with oxygen. We assume that the underlying substrate is at least partly responsible for the inertness of the clusters although the protection mechanism is not yet fully understood.

Acknowledgements

We thank the Ministerium für Wissenschaft und Forschung des Landes Nordrhein-Westfalen (Referat IV A5, D. Dzwonnek) and the Deutsche Forschungsgemeinschaft for financial support of our work which was partly carried out within the framework of the “Forschergruppe Modellkat”.

References

- [1] H. Poppa, Catal. Rev. Sci. Eng. 34 (1993) 129–178.
- [2] T. Wang, C. Lee, L.D. Schmidt, Surf. Sci. 163 (1985) 181.
- [3] S. Lijima, M. Ichikawa, J. Catal. 94 (1985) 313.
- [4] P. Gallezot, C. Lequerq, in: B. Imelik, J. Vedrine (Eds.), Catalysis Characterization, Plenum, New York, 1994, p. 521.
- [5] B.C. Gates, L. Guzzi, H. Knözinger (Eds.), Metal Clusters in Catalysis, Studies in Surface Science and Catalysis, vol. 29, Elsevier, Amsterdam, 1986.
- [6] R.M. Jaeger, H. Kuhlenbeck, H.-J. Freund, M. Wuttig, W. Hoffmann, R. Franchy, H. Ibach, Surf. Sci. 259 (1991) 235.
- [7] M. Wuttig, W. Hoffmann, R. Jaeger, H. Kuhlenbeck, H.-J. Freund, Mater. Res. Soc. Symp. Proc. 221 (1991) 143.
- [8] J. Libuda, M. Bäumer, H.-J. Freund, Th. Bertrams, H. Neddermeyer, K. Müller, Surf. Sci. 318 (1994) 61.
- [9] M. Bäumer, J. Libuda, H.-J. Freund, Metal deposits on thin well ordered oxide films: Morphology, adsorption and reactivity, in: R.M. Lambert, G. Pacchioni (Eds.), NATO Advanced Study Institute, NATO ASI Series E, Kluwer, Dordrecht, p. 61.
- [10] H.-J. Freund, Angew. Chem., Int. Ed. Engl. 36 (1997) 452.
- [11] A. Sandel, J. Libuda, P. Brühwiler, S. Anderson, M. Bäumer, A. Maxwell, N. Mårtensson, H.-J. Freund, J. Vac. Sci. Technol. A 14 (1996) 1546.
- [12] S. Wohlrab, F. Winkelmann, H. Kuhlenbeck, H.-J. Freund, Adsorption on epitaxial oxide systems as model systems for heterogeneous catalysis, in: R.J. McDonald, E.C. Taglauer, K. Wandelt (Eds.), Surface Science: Principles and Current Applications, Springer, Berlin, 1996, p. 193.
- [13] M. Klimenkov, S. Nepijko, H. Kuhlenbeck, M. Bäumer, R. Schlögl, H.-J. Freund, Surf. Sci. 391 (1997) 27.
- [14] M. Klimenkov, S. Nepijko, H. Kuhlenbeck, H.-J. Freund, Surf. Sci. 385 (1997) 66.
- [15] R.C. Weast (Ed.), CRC Handbook of Chemistry and Physics, 51st ed., CRC Press, Cleveland, OH, 1970.
- [16] K. Heinemann, H. Poppa, Surf. Sci. 156 (1985) 265–274.
- [17] J.C. Fuggle, N. Mårtensson, J. Electron Spectrosc. Relat. Phenom. 21 (1980) 275.
- [18] F.J. Himpsel, J.F. Morar, F.R. McFeely, R.A. Pollak, G. Hollinger, Phys. Rev. B 30 (1984) 7236.
- [19] G.K. Wertheim, Z. Phys. D 12 (1989) 319.
- [20] S.B. DiCenzo, G.K. Wertheim, Comments Solid State Phys. 11 (1985) 203.
- [21] J. Libuda, Ph.D. Thesis, Ruhr-Universität, Bochum, 1996.
- [22] M.W. Ruckman, S.-L. Qui, M. Strongin, Appl. Surf. Sci. 89 (1995) 401.